JAAS

PAPER

View Article Online
View Journal | View Issue

Cite this: *J. Anal. At. Spectrom.*, 2014, **29**, 1406

Precise measurement of chromium isotopes by MC-ICPMS

Martin Schiller,* Elishevah Van Kooten, Jesper C. Holst, Mia B. Olsen and Martin Bizzarro

We report novel analytical procedures allowing for the concurrent determination of the stable and mass-independent Cr isotopic composition of silicate materials by multiple collector inductively coupled mass spectrometry (MC-ICPMS). In particular, we focus on improved precision of the measurement of the neutron-rich isotope ^{54}Cr. Because nitride and oxide interferences are a major obstacle to precise and accurate ^{54}Cr measurements by MC-ICPMS, our approach is designed to minimize these interferences. Based on repeat measurements of standards, we show that the mass-independent ^{53}Cr and ^{54}Cr compositions can be routinely determined with an external reproducibility better than 2.5 and 5.8 ppm (2 sd), respectively. This represents at least a two-fold improvement compared to previous studies. Although this approach uses significantly more Cr (30–60 μg) than analysis by thermal ionization mass spectrometry (TIMS), our result indicate that it is possible to obtain an external reproducibility of 19 ppm for the μ^{54}Cr when consuming amounts similar to that typically analyzed by TIMS (1 μg). In addition, the amount of time required for analysis by MC-ICPMS is much shorter thereby enabling a higher sample throughput. As a result of the improved analytical precision, we identified small apparent mass-independent differences between different synthetic Cr standards and bulk silicate Earth (BSE) when using the kinetic law for the mass bias correction. These differences are attributed to the Cr loss by equilibrium processes during production of the synthetic standards. The stable isotope data concurrently obtained have a precision of 0.05‰ Da^{-1}, which is comparable to earlier studies. Comparison of the measured isotopic composition of four meteorites with published data indicates that Cr isotope data measured by the technique described here are accurate to stated uncertainties. The stable Cr composition of the Bilanga and NWA 2999 achondrites suggests that the differences in the stable Cr isotope composition of Earth and chondrites may reflect heterogeneity of their precursor material rather than Cr isotope fractionation during metal–silicate segregation of Earth. Lastly, a step wise dissolution experiment of the CI chondrite Ivuna reveals previously unknown carriers of large mass-dependent Cr stable isotope variations that co-vary with the known presence of carriers of large nucleosynthetic anomalies, demonstrating one advantage of this technique.

Received 14th January 2014
Accepted 8th April 2014

DOI: 10.1039/c4ja00018h

www.rsc.org/jaas

1 Introduction

Chromium has four naturally occurring isotopes – ^{50}Cr, ^{52}Cr, ^{53}Cr and ^{54}Cr – with relative abundances of 4.35%, 83.79%, 9.50% and 2.36%, respectively. Variations in the relative abundances of these isotopes in meteorites and the terrestrial rock record can be used to study processes associated with the formation and evolution of the earliest solar system as well as ancient and modern terrestrial environments (*e.g.*, ref. 1–4). In cosmochemistry, chromium is particularly useful because the abundance of ^{53}Cr and ^{54}Cr provides temporal and spatial information on early solar system processes (*e.g.*, ref. 1 and 5–7). Given that the documented Cr isotope variations are typically small, improving the precision of Cr isotope measurements can potentially allow for a better understanding of the processes that shaped our solar system.

Of the two Cr isotopes particularly relevant to cosmochemists, namely ^{53}Cr and ^{54}Cr, the neutron-rich ^{54}Cr nuclide is predominantly produced by neutron-rich statistical equilibrium or quasi-equilibrium processes occurring in a type Ia supernova.[8–10] In contrast, ^{50}Cr, ^{52}Cr, and ^{53}Cr are primarily the products of explosive oxygen and silicon burning in supernovae.[10] The major nucleosynthetic source of ^{54}Cr does not significantly synthesize the other Cr isotopes and, therefore, variable contribution from a ^{54}Cr producing source to the nascent solar system is not predicted to significantly modify the abundance of the remaining Cr isotopes. It is now firmly established that heterogeneity in ^{54}Cr/^{52}Cr ratios exists between different bulk solar reservoirs,[6] which is thought to reflect

Centre for Star and Planet Formation, Natural History Museum of Denmark, University of Copenhagen, DK-1350, Copenhagen, Denmark. E-mail: schiller@snm.ku.dk

admixing of variable amounts of pre-solar carriers heavily enriched in ^{54}Cr.[11,12] The presence of nucleosynthetic ^{54}Cr variability between different bulk solar system reservoirs provides a means to explore genetic relationships between early solar system condensates, diverse asteroids and the terrestrial planets.[6] However, the total range of known ^{54}Cr variability in bulk meteorites is limited to only ~250 ppm.[6] Thus, taking full advantage of potential ^{54}Cr variability to track genetic relationships between early solar system reservoirs requires highly-precise ^{54}Cr/^{52}Cr measurements.

A minor additional component to the nucleosynthesis of ^{53}Cr comes from the decay of the short-lived radionuclide ^{53}Mn.[13,14] With a half-life of 3.74 Ma, the ^{53}Mn–^{53}Cr decay system is a powerful chronometer to date asteroidal differentiation processes in the early solar system (*e.g.*, ref. 5, 15 and 16). However, the relatively low initial solar system ^{53}Mn/^{55}Mn ratio of $\sim 6 \times 10^{-6}$ (ref. 15) coupled with the relatively long half-life of the decay system results in ^{53}Cr excesses in bulk basaltic meteorites that are typically less than 150 ppm (*e.g.*, ref. 5). Thus, similarly to ^{54}Cr, improving measurements of the radiogenic ^{53}Cr component may allow for a refined chronology of early solar system events based on the ^{53}Mn–^{53}Cr system.

Precise measurement of the radiogenic and nucleosynthetic components of Cr isotopes in meteoritic materials has so far primarily been performed by thermal ionization mass spectrometry (TIMS). This approach allows for the analysis of small quantities of Cr on the order of 0.5–1 μg with a typical external reproducibility of 10–20 ppm for ^{54}Cr/^{52}Cr ratios,[5,17–20] making the uncertainty a limiting factor in the resolution of potential small differences between distinct reservoirs. Moreover, significant improvement in Cr isotope measurements beyond the current state-of-the-art is limited by complications inherent to TIMS analyses such as, for example, filament poisoning and reservoir fractionation effects (*e.g.*, ref. 21). In contrast, isotope ratio measurements by multiple collector inductively coupled plasma mass spectrometry (MC-ICPMS) may allow for significant improvement in reproducibility owing to the sample-standard bracketing technique. Indeed, recent studies have demonstrated that it is possible to obtain external reproducibilities below 5 ppm for the analysis of internally normalized Mg and Ca isotope ratios of chemically purified silicate matrices by MC-ICPMS.[22–26] Although some attempts have already been conducted to measure nucleosynthetic and radiogenic isotope effects on ^{53}Cr and ^{54}Cr by MC-ICPMS,[16,27] the external reproducibility of these measurements has not been significantly improved compared to typical TIMS measurements. This primarily stems from the presence of irresolvable isobaric interferences that affect the Cr mass array resulting from residual impurities in the Cr analyte solution such as, for example, ^{50}Ti, ^{50}V and ^{54}Fe. Corrections for these isobaric interferences are much more important in MC-ICPMS work compared to TIMS given the high ionization efficiency of the plasma source. Additional isobaric interferences from molecular species include argon nitride (^{40}Ar^{14}N) and oxide (^{40}Ar^{16}O), which affect mass ^{54}Cr and ^{56}Fe, respectively. Appropriate monitoring of the ^{56}Fe peak is critical to correct for any remaining Fe in the Cr solution that may affect the measured ^{54}Cr abundance *via* a direct isobar from ^{54}Fe. Therefore, it is apparent that a prerequisite to high-precision Cr isotope analysis by MC-ICPMS is the efficient removal of interferences and careful assessment of the accuracy of applied corrections.

Here we describe a novel analytical approach utilizing MC-ICPMS that addresses these issues and allows us to measure the nucleosynthetic and radiogenic isotope effects on ^{53}Cr and ^{54}Cr to a precision that is comparable to traditional TIMS analysis for similar sized samples and offers a significant improvement where the sample is not limited. In addition, this approach allows for concurrent determination of the stable Cr isotopic composition of the sample allowing for better quality assessment of the data.

2 Analytical methods

2.1 Chromium separation from the sample matrix

Chromium occurs in nature either as trivalent Cr(III) or hexavalent Cr(VI). The difference in valance state affects the ion chromatographic properties of Cr, which is commonly utilized to separate the two species (*e.g.*, ref. 28). Therefore, to maximize total Cr yields, care was taken to ensure the conversion of all Cr into the required oxidation state prior to each chemical separation step. We describe below a four step column chromatographic procedure (summarized in Table 1) aimed at providing high Cr yields and efficient purification from matrix elements.

Table 1 Four step Cr purification scheme for a 10 mg silicate sample

Eluent	Vol.[a] (mL)	Elements eluted
Step 1: Fe removal[b]		
6 M HCl	2	Conditioning
Load sample in 6 M HCl	1	
6 M HCl	2	Cr + matrix
Remaining on column		Fe
Step 2: matrix removal[c]		
0.5 M HCl	4	Conditioning
Load sample in 0.5 M HCl	3	
0.5 M HNO_3	20	Cr
6 M HCl	10	Matrix
Step 3: Ti removal[d]		
14 M HNO_3	4	Conditioning
Load sample in 14 M HNO_3	0.5	
14 M HNO_3	4	Cr
Step 4: V removal[d]		
8 M HCl	4	Conditioning
Load sample in 8 M HCl	0.5	
8 M HCl	2	Cr

[a] Volume of the eluent. [b] Biorad poly-prep column with 2 mL AG1-X4 200–400 mesh resin. [c] Biorad poly-prep column with 2 mL of AG50W-X8 200–400 mesh resin. [d] Pipette tip column with 0.75 mL of TODGA resin. All resins are discarded after use.

First, all samples were purified for Fe by passing the sample through AG1-X4 200–400 mesh anion resin in 6 M HCl (Table 1). The resin bed was typically 2 mL for sample sizes of 50 mg. Cr was collected with the initial load and an additional 4 mL of 6 M HCl.

In a second step, total sample equivalents of 10 mg were passed through ~2 mL of BioRad AG50W-X8 200–400 mesh resin. For larger samples, volumes were scaled accordingly. In preparation of this separation step, samples were fluxed for 12 h in 6 M HCl to convert Cr to its trivalent form. The solution was diluted then to 0.5 M HCl with distilled water and loaded onto the resin. The Cr cut was collected in the initial load and an additional 20 mL of 0.5 M HNO_3. The remaining matrix was eluted from the column in 10 mL 6 M HCl. To ensure near complete recovery of Cr in this step, the eluted matrix was collected and reprocessed through the same column and the Cr cuts from both elutions were combined.

Remaining trace amounts of Ti and V were specifically targeted in the last two separation steps using Eichrom TODGA resin. The first TODGA resin step utilizes the high retention of Ti on the resin in concentrated HNO_3, while the second step takes advantage of the retention of V in 8 M HCl.[29] Samples were loaded onto a 0.75 mL resin bed in a pipette tip column in 0.5 mL 14 M HNO_3 and Cr was collected in the load and an additional 4 mL of 14 M HNO_3. Subsequently the resin was cleaned by alternate washing with distilled water, 6 M HCl and 7 M HNO_3. Following this step, the Cr fraction was converted into chloride form and loaded in 0.5 mL 8 M HCl onto the same resin bed. The Cr was collected with the load and an additional 2 mL of 8 M HCl.

Because any remaining trace of Fe in the sample requires significant interference corrections on ^{54}Cr, samples were passed through a final anion chemistry identical to the first Cr separation step but using a smaller resin bed and elution volume of 0.25 mL and 3 mL, respectively. Each sample was monitored prior to analysis by MC-ICPMS for Fe concentration and samples that required more than 100 ppm correction on ^{54}Cr from ^{54}Fe were re-processed through the Fe separation step. Total procedural blanks of this procedure were on the order of a few ng of Cr and inconsequential considering the size of the samples and their Cr isotopic anomalies.

2.2 Chromium isotope measurements by MC-ICPMS

Chromium data were acquired with the ThermoFisher Neptune Plus MC-ICPMS located at the Centre for Star and Planet Formation (Natural History Museum of Denmark, University of Copenhagen). Because the gas based $^{40}Ar^{16}O$ and $^{40}Ar^{14}N$ interferences increase significantly when using high sensitivity cones such as the Jet sample cone and the skimmer X-cone offered by ThermoFisher, a lower sensitivity approach was taken by combining a Jet sample cone with a skimmer H-cone. This lowers the sensitivity by about 30% compared to a Jet sample cone and skimmer X-cone, but reduces oxide and nitride interferences by a factor of at least 2–3. To further reduce these interferences, samples were introduced into the plasma in 2.5% HNO_3 *via* an ESI Apex IR desolvating nebulizer with trifluoro-methane (CHF_3) as the supplementary gas instead of using N_2. Although the introduction of carbon creates a significant $^{40}Ar^{12}C$ interference on ^{52}Cr, the gas significantly reduces the nitride and oxide interferences and has a positive influence on overall signal sensitivity and stability. Optimal sensitivity combined with minimal oxide and nitride production was achieved by running in 'cold plasma' mode with an RF power of 600 to 800 W depending on daily tuning conditions. Under these analytical conditions, the $^{40}Ar^{16}O$ and $^{40}Ar^{14}N$ signals were typically below 0.5 V and 0.2 V, respectively, when using the high (16 μm) resolution slit of the Neptune. With this setup and a sample aspiration rate of ~60 μL min^{-1}, a concentration of 1 ppm resulted in a ^{52}Cr signal of ~30 V.

Chromium isotope data were acquired in static mode using seven Faraday collectors. Apart from the four Cr isotopes (^{50}Cr, ^{52}Cr, ^{53}Cr, ^{54}Cr), ^{49}Ti, ^{51}V and ^{56}Fe were also monitored to correct for unresolvable isobaric interferences on ^{50}Cr from ^{50}Ti and ^{50}V as well as on ^{54}Cr from ^{54}Fe. Faraday collectors were connected with 10^{11} Ω feedback resistors for ^{50}Cr, ^{53}Cr, ^{54}Cr and ^{51}V. The largest beam ^{52}Cr was monitored using a 10^{10} Ω feedback resistor to allow for beam intensities larger than 50 V whereas low noise 10^{12} Ω feedback resistors were used for measurement of the small ^{49}Ti and ^{56}Fe signals. Data were acquired on the low mass side of the Cr peak typically at a centre mass of 51.910 or ~0.030 atomic mass units (Da) from the peak centre using the 16 μm entrance slit with a resolving power ($M/\Delta M$ as defined by the peak edge width from 5–95% full peak height) that was always greater than 8000 for ^{54}Cr to ensure a interference-free peak flat plateau. At this given resolution, this peak position allows the collection of carbide, oxide and nitride interference-free signals for all Cr isotopes as well as ^{49}Ti, ^{51}V, and ^{56}Fe (Fig. 1).

Peak centres were performed only at the beginning of an analytical session and no peak drift was observed for sessions lasting more than 48 h. Because the Neptune peak centre routine was applied to the ^{52}Cr signal, which also comprised of a 5–10% $^{40}Ar^{12}C$ interference signal, slight differences in the peak centre position exist between different analytical sessions. Therefore, after determining the peak centre position, the position of the interference-free plateau was determined by measuring the Cr isotopic ratios across the low mass side of the Cr peak at different individual mass positions prior to each analytical sessions in a similar fashion as described by Weyer and Schwieters (2003).[30] Based on this experiment, an ideal mass position for analysis was determined and used for the remainder of individual analytical sessions.

Samples were typically analysed at a ^{52}Cr signal intensity of 100 V and beam intensities of standard and sample were matched within 5% of each other. Each analysis comprised a total of 1259 s of combined wash out and baseline measurements obtained on-peak (in the same 2.5% HNO_3 solution used to dissolve samples and standards) and 1667 s of data acquisition (100 scans integrated over 16.67 s). In between each step the auto sampler probe was cleaned for 30 s in a rinse solution of the same molarity. From the 1259 s of data

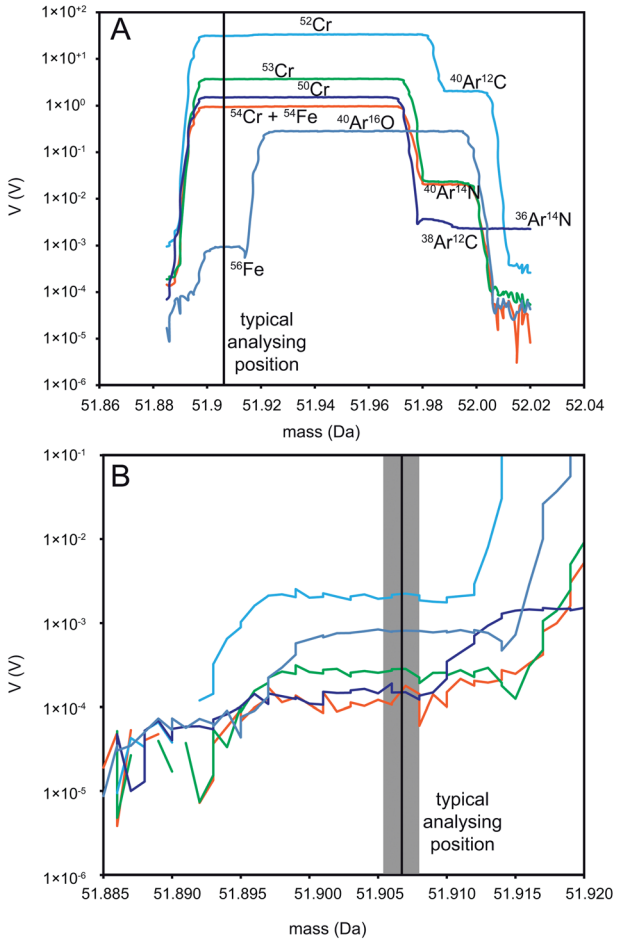

Fig. 1 In (A) a typical peak scan of the Cr isotopes and ^{56}Fe is shown with approximately 20 V on the ^{52}Cr signal and when measuring under the analytical conditions described in the text. (B) depicts the interference area of the Cr peak at the low mass end when measuring the blank solution. Indicated in both figures is the approximate mass position at which the isotopic measurement was typically conducted.

collected in the on-peak zero solution, only the last 800 s were used as baseline measurement. This approach allowed close monitoring of the wash out behaviour of the sample and standard. Where sufficient Cr is available, samples were systematically analysed 10 times over a time span of ~18 h consuming a total of 30 to 60 μg Cr.

2.3 Data reduction

All data reductions were conducted off-line using the freely available Iolite[31] data reduction software that runs within Igor Pro. The Cr data reduction module used for the data reported here can be freely obtained from the authors on request. Background intensities were interpolated using a smoothed cubic spline, as were changes in mass bias with time. Iolites 'Smooth spline auto' choice was used in all cases, which determines a theoretically optimal degree of smoothing based on variability in the reference standard throughout an analytical session. For all reported data the baseline subtraction was conducted using the 'automatic' spline option of Iolite, while standard interpolation was done using the 'smooth spline auto' option. Stable isotope ratios are reported in the δ notation according to the following formula:

$$\delta^{X}\mathrm{Cr}\,[‰] = \left[\frac{(^{X}\mathrm{Cr}/^{52}\mathrm{Cr})_{\mathrm{sample}}}{(^{X}\mathrm{Cr}/^{52}\mathrm{Cr})_{\mathrm{SRM979}}} - 1\right] \times 10^{3} \quad (1)$$

where x is either 50, 53 or 54. The mass-independent component of ^{53}Cr (μ^{53}Cr) and ^{54}Cr (μ^{54}Cr) is reported in the same fashion, but in the μ notation as parts per million (ppm) instead of parts per thousand (‰). We use mass-independent as a generic term to describe radiogenic ingrowth on ^{53}Cr, nucleosynthetic anomalies on ^{54}Cr or, alternatively, inappropriate mass fractionation correction on both ^{53}Cr and ^{54}Cr. However, we emphasize that latter is in fact an apparent mass-independent effect, as it reflects an artefact of using an inappropriate mass fractionation law to account for a mass dependent process. The reported mass-independent component is the deviation from the internally normalized ^{53}Cr/^{52}Cr and ^{54}Cr/^{52}Cr of the sample from the reference standard (SRM 979), normalized to a ^{50}Cr/^{52}Cr = 0.051859 (ref. 32) using the exponential mass fractionation law.

3 Discussion

3.1 Reduction of gas based interferences

A major challenge when measuring Cr isotopes with an Ar-based plasma is the isobaric molecular interference resulting from the Ar gas. In particular, ^{40}Ar^{16}O and ^{40}Ar^{14}N are troublesome because they produce interference on the masses 54 and 56 and, thus, resolving these interferences is necessary for acquiring precise and accurate ^{54}Cr data. As such, we focused on minimizing the contribution of molecular argon species to the Cr mass array. This was achieved by taking several steps. (1) Instead of using the highest sensitivity sample introduction sampler and skimmer cone setup of the Neptune Plus, a combination of the Jet and X-cone, we opted for a somewhat less sensitive combination of the Jet sampler cone and H skimmer cone. This results in at least 30% sensitivity loss for the Cr signal, but reduces the oxide and nitride production rate by a factor of 2–3, effectively improving the sample over oxide and nitride signal. (2) Reduction of the RF power has long been known to be an effective mechanism to reduce the oxide production rate (*e.g.*, ref. 33). In the case of our approach measuring Cr isotopes, a lower RF power of 700 W compared to the usually applied 1200 W also resulted in a slight sensitivity improvement of the Cr signal of 10 to 20%, while suppressing the oxide and nitride production by a factor of (~2–3). Finally, the usual additive gas of the apex sample introduction system is N_2. While addition of an additive gas is not essentially required, it does improve signal stability and can enhance the sensitivity of the system. However, considering that one of the biggest challenges in measuring a precise ^{54}Cr signal is resolving the ^{40}Ar^{14}N interference, unnecessary addition of N_2 is counterproductive. To circumvent this problem, we turned to trifluoromethan (CF_3H) as an additive gas. A positive effect on the reduction of molecular interferences through the addition of

CF_3H to the Ar plasma has previously been reported[34] and can also be observed for $^{40}Ar^{14}N$ and $^{40}Ar^{16}O$. However, the additional introduction of CF_3H produces also a significant $^{40}Ar^{12}C$ interference on mass 52. Fortunately, this interference requires the lowest mass resolving power of the three discussed molecular interferences and it is also an isobar on the most abundant Cr isotope, which results in a favourable signal to isobar ratio. The $^{40}Ar^{12}C$ signal was typically between 5 and 15 V compared to a ^{52}Cr signal of 40 to 100 V. When using the high or medium resolution slits of the Neptune Plus, it is possible to obtain an interference-free plateau of 5 to 10 milli mass units on the low mass side of the peak. The position of and centre of this plateau were determined prior to each analytical session.

3.2 Correction of atomic isobaric interferences

Because the Ar plasma has a very high ionization efficiency, another critical step in acquiring accurate Cr isotope data by MC-ICPMS is an effective correction for the atomic isobaric interferences ^{49}Ti, ^{51}V, and ^{56}Fe, which cannot be resolved. The effect of these isobars is slightly different because the presence of Ti and V interferes with the mass bias correcting isotope ^{50}Cr and affects all measured Cr isotope ratios, while the presence of Fe solely affects the ^{54}Cr data. In order to test the accuracy of the interference corrections, a Cr ICPMS standard solution was doped separately with Ti, V and Fe at a level significantly larger than that of any sample after chemical Cr purification.

For Ti, the ^{50}Ti interference was subtracted from ^{50}Cr by calculating a mass-bias corrected ^{50}Ti signal from the measured ^{49}Ti beam. For mass-bias correction a $^{50}Ti/^{49}Ti = 0.97377$ (ref. 35) was inferred and the fractionation factor was derived from the $^{53}Cr/^{52}Cr$-ratio that is free of isobaric interferences using a natural ratio of 0.11339 assuming a negligible difference in the mass fractionation behaviour of Ti and Cr. Because ^{53}Cr can be affected by the decay of ^{53}Mn, this correction scheme is only robust for samples with small Mn/Cr ratios (and ^{53}Cr anomalies of less than a few hundred ppm) or that formed after extinction of ^{53}Mn (such as all terrestrial rocks). For samples where ^{53}Cr anomalies are significant and result in noticeable effects in the mass bias correction, an iterative approach can be taken with an initial correction of ^{50}Cr and then a secondary mass bias correction using the preliminary corrected $^{50}Cr/^{52}Cr$-ratio for precise determination of the size of the ^{50}Ti interference.

The Ti correction was tested by measuring a Cr solution containing a contribution of ^{50}Ti of more than 1609 ppm to the ^{50}Cr signal (Table 2), which is at least a factor of ten larger than that measured for natural samples processed through the Cr purification, *versus* the pure Cr solution. Prior to the interference correction this amount of Ti resulted in apparent excesses in the mass bias corrected $\mu^{53}Cr$ and $\mu^{54}Cr$ of +777.2 and +1532.2, respectively. After correction both $\mu^{53}Cr$ and $\mu^{54}Cr$ were +1.2 ± 2.2 and +3.6 ± 2.6 (uncertainties are 2 se if not stated otherwise), respectively, within an analytical uncertainty of zero when considering the external reproducibility of our approach (see below). Given the fact that the Ti concentration in this test exceeds that of typical samples after Cr purification by more than one order of magnitude, we feel confident that no bias during sample analysis is introduced from the Ti correction.

The correction of a potential vanadium contribution to the ^{50}Cr signal was conducted by calculating a ^{50}V signal based on ^{51}V assuming a natural $^{50}V/^{51}V$ of 2.425×10^{-3} (ref. 36). The correction of mass bias experienced by ^{51}V in the MC-ICPMS and signal subtraction of the calculated ^{50}V beam contributing to ^{50}Cr was done in the same manner as for Ti. A similar V interference test as for Ti was conducted to verify the accuracy of the approach. For this a Cr solution containing a ~24 ppm contribution of ^{50}V to the ^{50}Cr signal was measured *versus* a pure Cr solution (Table 2). The tested V contribution is much smaller than that of the Ti test given the much lower natural abundance of the ^{50}V isotope ($^{51}V/^{50}V \sim 400$). As a result, the apparent excesses on both $\mu^{53}Cr$ and $\mu^{54}Cr$ of +10.2 ± 2.6 and +24.9 ± 2.9, respectively, are also small but resolvable. No apparent excesses remained after the V correction with a $\mu^{53}Cr$ and $\mu^{54}Cr$ of −0.4 ± 2.1 and −0.3 ± 1.7, respectively (Table 2).

Lastly, the correction for the isobaric Fe interference on ^{54}Cr was tested. The correction for any contribution of ^{54}Fe to the ^{54}Cr signal is non-trivial because the geometry of the Neptune Plus does not allow the measurement of the relatively interference-free ^{57}Fe simultaneously with all Cr isotopes and ^{49}Ti. Instead this correction must be based on ^{56}Fe. A Fe correction using ^{56}Fe is complicated by the typically large isobaric $^{40}Ar^{16}O$ interference and hence requires careful assessment. While the mass resolution of the Neptune does in principle allow the full resolution of ^{56}Fe and $^{40}Ar^{16}O$, the interference is significantly larger by orders of magnitude than the ^{56}Fe signal. Thus, even small tailing contributions of $^{40}Ar^{16}O$ can lead to overcorrection and additional noise in the calculated ^{54}Fe signal. Because no Fe isotope interferes with the ^{50}Cr and ^{52}Cr signals, the contribution of ^{54}Fe to the ^{54}Cr signal was calculated using a Ti and V corrected $^{50}Cr/^{52}Cr$ for mass bias correction and a natural isotope abundance fraction of 0.05845 and 0.91754 for ^{54}Fe and ^{56}Fe, respectively.[37] Similar to the tests for Ti and V, a pure Cr solution was doped with Fe at a level that significantly exceeds that of purified Cr samples and was measured *versus* a pure

Table 2 Summary of interference correction tests performed on the pure SRM 979 Cr standard doped with single element solutions of Ti, V, and Fe. Shown uncertainties are the 2 se of the replicate analyses

Isobar	Inf. contrib. (ppm)	$\mu^{53}Cr_{uncor}$ (ppm)	$\mu^{54}Cr_{uncor}$ (ppm)	$\mu^{53}Cr_{cor}$ (ppm)	$\mu^{54}Cr_{cor}$ (ppm)	n
^{50}Ti	1609.2	+777.2 ± 2.0	+1532.2 ± 2.1	+1.2 ± 2.2	+3.6 ± 2.6	10
^{50}V	23.6	+10.2 ± 2.6	+24.9 ± 2.9	−0.4 ± 2.1	−0.3 ± 1.7	10
^{54}Fe	558.1	+1.4 ± 1.8	+555.7 ± 4.6	+1.7 ± 2.1	+1.2 ± 2.3	10

solution to test the accuracy of the applied correction. In the test, the ^{54}Fe contribution to the ^{54}Cr signal was calculated to be 558.1 ppm, compared to typically less than 50 ppm for purified Cr samples. Prior to the interference correction, this resulted in an apparent excess on μ^{54}Cr of +555.7 ± 4.6 that was fully corrected for to +1.2 ± 2.3 through the Fe-subtraction. At this iron concentration, the interference correction is also the only one of the tested atomic interferences where the uncertainty in the isotope ratio used for correction has a quantifiable effect (3 ppm) on the final corrected μ^{54}Cr and could potentially introduce a bias to the data. However, the successful correction to within uncertainty of zero demonstrates that even large contributions of Fe to the Cr signal can be completely corrected for and no resolvable bias is introduced in the calculated μ^{54}Cr composition by the applied isotope ratios for interference correction.

3.3 Reproducibility and comparison with previous data

3.3.1 Cr stable isotope data. High precision chromium stable isotope data have already been routinely collected by MC-ICPMS (*e.g.*, ref. 38–40). Based on all repeat measurements presented in this study (Table 3), the sample-standard bracketing approach taken here results in a similar reproducibility of 0.05‰ Da^{-1} compared to that of studies using either standard-sample bracketing 39 or the use of a Cr double spike 38. The δ^{53}Cr offset of −0.152 ± 0.045 for the DTS-2B dunite standard with respect to SRM 979 is in excellent agreement with that of terrestrial igneous silicates of −0.124 ± 0.101 determined by Schönberg *et al.*[38] The δ^{53}Cr of −0.290 ± 0.010 and −0.310 ± 0.010 for the CI chondrite Ivuna and the H6 chondrite Portales Valley, respectively, analysed here are also in good agreement with that of the average carbonaceous [−0.31 ± 0.11 (2 sd)] and ordinary [−0.20 ± 0.13 (2 sd)] chondrites (Fig. 2).[40]

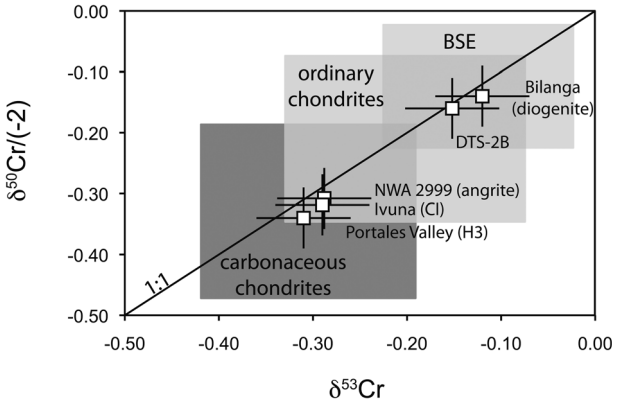

Fig. 2 Stable isotope data (δ^{53}Cr and δ^{50}Cr normalized to represent one atomic mass unit difference from the normalizing isotope) for meteorites compared with those of published values. Data for BSE are from (ref. 38) and those for ordinary and carbonaceous chondrites were taken from (ref. 40).

The δ^{53}Cr composition of the diogenite Bilanga (−0.120 ± 0.010) is indistinguishable from that of DTS-2B and bulk silicate Earth (BSE; Fig. 2). In contrast, the NWA 2999 angrite has a lighter δ^{53}Cr of −0.288 ± 0.027, which is comparable to chondrites. The compositional difference between Bilanga and NWA 2999, which are both products of differentiated planetesimal, is surprising because an isotopically heavier stable Cr composition of BSE with respect to chondrites has been used to argue for Cr isotope fractionation during low temperature parent body differentiation on planetary embryos.[40] In particular, Moynier *et al.* suggested that the oxygen fugacity may play a role in the isotopic fractionation with higher fugacity imparting larger isotopic fractionation during metal–silicate differentiation. This, however, is not supported by the stable isotopic

Table 3 Stable and mass-independent Cr isotope data for standards and meteorites. Shown uncertainties are the 2 se of the replicate analyses

Sample	Type	δ^{50}Cr (‰)	δ^{53}Cr (‰)	δ^{54}Cr (‰)	μ^{53}Cr (ppm)	μ^{54}Cr (ppm)	*n*	^{55}Mn/^{52}Cr
***vs.* Peak performance:**								
Cr peak perf.	Cr standard	+0.003 ± 0.007	−0.003 ± 0.003	−0.002 ± 0.006	−1.2 ± 2.2	+1.0 ± 2.5	10	—
Cr + Ti peak perf.	Cr standard	−0.017 ± 0.031	+0.008 ± 0.015	+0.019 ± 0.030	+1.2 ± 2.2	+3.6 ± 2.6	10	—
Cr + V peak perf.	Cr standard	+0.018 ± 0.006	−0.009 ± 0.003	−0.018 ± 0.008	−0.4 ± 2.1	−0.3 ± 1.7	10	—
Cr + Fe peak perf.	Cr standard	+0.020 ± 0.012	−0.007 ± 0.007	−0.017 ± 0.012	+1.7 ± 2.1	+1.2 ± 2.3	10	—
Average and 2 sd		*+0.006 ± 0.034*	*−0.003 ± 0.015*	*−0.002 ± 0.034*	*+0.3 ± 2.7*	*+1.4 ± 3.3*	*4*	—
***vs.* SRM 979:**								
Cr peak perf.	Cr standard	−0.340 ± 0.039	+0.160 ± 0.020	+0.310 ± 0.041	−9.0 ± 2.2	−20.3 ± 4.2	10	—
Cr peak perf.	Cr standard	−0.327 ± 0.047	+0.150 ± 0.023	+0.300 ± 0.049	−8.0 ± 1.4	−16.9 ± 1.8	10	—
Cr peak perf.	Cr standard	−0.323 ± 0.043	+0.152 ± 0.022	+0.299 ± 0.045	−6.4 ± 1.6	−14.5 ± 2.7	10	—
Average and 2 sd		*−0.330 ± 0.018*	*+0.154 ± 0.011*	*+0.303 ± 0.012*	*−7.8 ± 2.6*	*−17.2 ± 5.8*	*3*	—
DTS-2B 1	Dunite	+0.325 ± 0.008	−0.156 ± 0.003	−0.307 ± 0.010	+3.5 ± 1.1	+8.4 ± 3.2	10	—
DTS-2B 2	Dunite	+0.385 ± 0.009	−0.183 ± 0.003	−0.360 ± 0.010	+3.6 ± 2.0	+8.9 ± 3.0	10	—
DTS-2B 3	Dunite	+0.276 ± 0.019	−0.132 ± 0.010	−0.270 ± 0.017	+3.4 ± 1.5	+3.8 ± 4.1	10	—
DTS-2B 4	Dunite	+0.294 ± 0.013	−0.139 ± 0.008	−0.274 ± 0.013	+4.8 ± 1.5	+10.4 ± 2.8	10	—
Average and 2 sd		*+0.320 ± 0.096*	*−0.152 ± 0.045*	*−0.303 ± 0.083*	*+3.8 ± 1.3*	*+7.9 ± 5.7*	*4*	—
Ivuna	CI	+0.637 ± 0.019	−0.290 ± 0.010	−0.445 ± 0.011	+16.4 ± 2.0	+155.2 ± 4.8	10	0.748 ± 0.003
Portales Valley	H	+0.680 ± 0.010	−0.310 ± 0.010	−0.690 ± 0.010	+15.2 ± 2.0	−39.4 ± 4.0	10	0.797 ± 0.004
Bilanga	Diogenite	+0.280 ± 0.010	−0.120 ± 0.010	−0.340 ± 0.010	+15.0 ± 2.4	−62.6 ± 3.8	10	0.653 ± 0.002
NWA 2999	Angrite	+0.616 ± 0.054	−0.288 ± 0.027	−0.640 ± 0.053	+10.2 ± 2.2	−49.5 ± 4.5	10	0.802 ± 0.003

composition of the Bilanga and NWA 2999 meteorites coupled with estimates of the oxygen fugacity during angrite and eucrite formation, which appear to have been more oxidising on the angrite parent body.[41] Considering that no single type of chondrite can explain the chemical and isotopic composition of the Earth,[42] this suggests that differences in the stable isotopic composition of Cr between meteorites and Earth are not predominantly controlled by metal–silicate fractionation but are instead the product of differences in the stable isotopic composition of their precursor material. This scenario is apparently consistent with the lack of Cr isotope homogenisation amongst bulk solar system reservoirs as evidenced by the presence of widespread ^{54}Cr nucleosynthetic heterogeneity.[6] In agreement with earlier work,[39] we conclude that accurate and reproducible stable Cr isotope data can be obtained by standard-sample bracketing using MC-ICPMS. Moreover, the lack of an isotopically enriched spike in our approach offers the possibility to concurrently determine stable, radiogenic and nucleosynthetic isotope effects, which are of particular interest in cosmochemistry.

3.3.2 Mass-independent data. As discussed earlier, the mass-independent compositions of ^{53}Cr (μ^{53}Cr) and ^{54}Cr (μ^{54}Cr) are of particular interest in meteoritic materials as they provide time information and trace potential genetic relationships amongst early solar system reservoirs, respectively. Thus, improving the precision and accuracy of μ^{53}Cr and μ^{54}Cr data is the focus of the technique described here. The external reproducibility was determined by repeated analysis of a pure Cr ICPMS standard solution (peak performance) and Cr chemically purified from the USGS dunite DTS-2B rock standard, which were both measured against the SRM 979 Cr isotopic standard. However, the peak performance and SRM 979 standards contained traces of Fe at a concentration equivalent to a few hundred ppm correction on ^{54}Cr. Thus, the SRM 979 was purified for Fe through step 1 of the Cr separation procedure described here. No such clean up was conducted for the peak performance Cr standard as this was used as an additional measure to test the reproducibility of a 'dirty' sample. However, we emphasize that the traces of Fe present in the peak performance standard are in much greater concentration (by a factor of ~10) compared to that remaining in the natural samples analyzed in this study. Repeated analysis of the peak performance Cr ICPMS solution including the contaminant tests with variable concentrations of interfering elements *versus* a pure peak performance solution ($n = 4$) resulted in μ^{53}Cr and μ^{54}Cr of +0.3 ± 2.7 (2 sd) and +1.4 ± 3.3 (2 sd), respectively, indistinguishable from zero. While this represents near ideal conditions (no chemical separation procedure), it offers an indication of the best possible accuracy that can be obtained by MC-ICPMS using the analytical conditions employed in this study.

The Cr peak performance solution was also measured *versus* the purified SRM 979 standard. This test reveals a difference in the stable isotopic composition of δ^{53}Cr = +0.154 ± 0.011 between these two standard solutions (Table 3). Further, when the kinetic (=exponential) law is used for the correction of mass discrimination experienced by the standard solutions a difference in μ^{53}Cr = −7.8 ± 2.6 and μ^{54}Cr = −17.2 ± 5.8 is obtained, indicating that the law used for mass discrimination is not appropriate to correct for the stable isotope difference between these two standards.[43] The stable isotope fractionation between the two standards is better, but not perfectly, described by a mass-dependence that follows the equilibrium law, which results in μ^{53}Cr = −3.2 ± 2.6 and μ^{54}Cr = −4.2 ± 5.8. These μ^{53}Cr and μ^{54}Cr values indicate that the difference in the stable isotope compositions between the two standards reflects predominantly variable equilibrium isotope fractionation during the production of the standards. When comparing the isotopic composition of both SRM 979 and peak performance standards to DTS-2B, which is a good representation of the Cr isotopic composition of BSE, it is evident that both standards experienced equilibrium isotope fractionation but to a variable degree (Table 3). Importantly, the different stable isotope compositions and the systematic offset between DTS-2B and SRM 979 of μ^{53}Cr = 3.8 ± 1.3 and μ^{54}Cr = 7.9 ± 5.7 can also, in part, be explained by loss of Cr through an equilibrium process experienced by SRM 979 during its production. The presence of resolvable fractionation effects in the Cr standards highlights the significance of the precise and accurate isotopic characterization of the Cr isotope standard used in future studies. For example, although this issue has recently been recognized,[18] little attention has been paid to the isotopic composition of the Cr standard used for comparison to meteoritic samples in earlier studies,[5,6,17,27,44,45] allowing for potential biases in the data and complicating a detailed comparison.

The most reliable assessment of the external reproducibility of our technique comes from measurements of Cr purified from multiple individually processed aliquots of the DTS-2B standard *versus* SRM 979 (Table 3). In fact, the reproducibility obtained for these samples is similar to or better than that achieved for repeat measurements of pure standard solutions, indicating that no variable bias was introduced through the chemical purification procedure. In combination with all repeat measurements of Cr standards performed in this study, the repeated analyses of DTS-2B indicate that it is possible to achieve an external reproducibility that is better than 2.5 and 5.8 for μ^{53}Cr and μ^{54}Cr, respectively. This represents a two-fold improvement compared to all earlier published work.

To further assess the accuracy of our approach, we also measured the Cr isotopic composition of four meteorites that have a known range of nucleosynthetic ^{54}Cr anomalies.[6,18,20] Within uncertainties, all four samples have ^{54}Cr anomalies that are in agreement with the published data. A good correlation and no resolvable systematic bias between the new high precision data and previously published data for the same meteorite or class of meteorite exists (Fig. 3), suggesting that our measurements are accurate to the stated uncertainties for samples with very distinct matrices.

Comparison of μ^{53}Cr for the analysed meteorites is complicated by differences in the standards used, secondary corrections in older literature and divergent ^{55}Mn/^{53}Cr ratios. Previous data for CI chondrites appear to be bimodal with average values of ~+23 (ref. 15 and 18) and ~+43 (ref. 16 and 20) for reasons that are not clear but could be related to distinct Cr isotopic

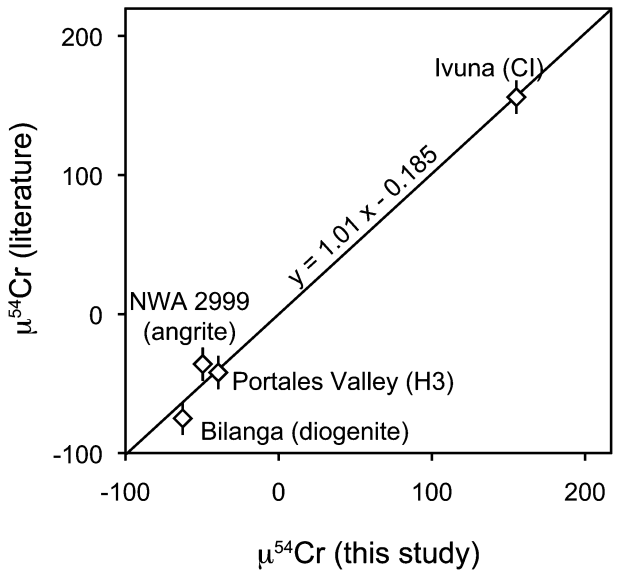

Fig. 3 Comparison of measured ^{54}Cr for different meteorites with that published for the same type of meteorite. Also shown is a linear fit to the data approximating a 1 : 1 correlation. Data from (ref. 6).

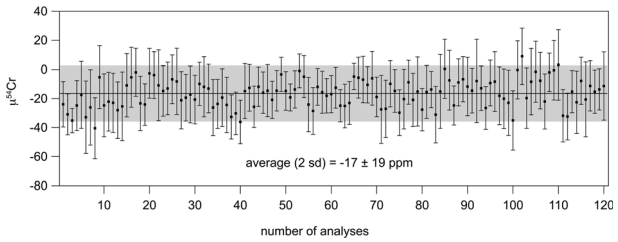

Fig. 4 Data for $\mu^{54}Cr$ from three individual measurements of peak performance ICPMS Cr standard solution *versus* SRM 979 (Table 3) shown as individual measurements of 415 s of data acquisition or representing ~1 μg Cr consumed during each analysis. Indicated in grey is the 2 sd of all data.

compositions of the respective standards used (*e.g.*, ref. 18). Our value of +16.4 ± 2.0 for the CI chondrite Ivuna is at the lower range of the lower estimates for this type of meteorite. However, we also measured a $^{55}Mn/^{53}Cr$ for our sample that is slightly lower (~15%) than the inferred bulk rock composition of this meteorite. Therefore, our data for Ivuna agrees well with that for the same type of meteorite determined by[15,18] but not with that of.[16,20] Very good agreement of the measured $\mu^{53}Cr$ exists for the H chondrite Portales Valley and the diogenite Bilanga with published values for meteorites of the same type.[15,18] No published $\mu^{53}Cr$ bulk data for NWA 2999 is available, although the smaller $\mu^{53}Cr$ excess compared to Bilanga is apparently consistent with the relatively young age of this angrite.[46]

3.4 Precision for small sample sizes

The high-precision Cr isotope analysis described here takes advantage of the relatively high Cr concentration of bulk meteorites and, therefore, large amounts of Cr are typically available for analysis. However, when aiming to analyse, for example, individual components in chondrites such as chondrules or refractory inclusions, the amount of available Cr is generally only in the order of a few μg or less. For such sample sizes, traditional TIMS measurements are well-suited although each individual measurement with uncertainties of ~20 ppm on ^{54}Cr requires several hours of machine time. On the other hand, single sample analysis of our method consumes between 3–6 μg of Cr, but results in uncertainties of ~10 ppm within ~1.5 hours when including the bracketing standard analyses. Thus, the MC-ICPMS potentially provides a much higher throughput of samples with comparable reproducibility.

To evaluate the external reproducibility of our methods for small sample sizes, we reprocessed our peak performance *versus* SRM 979 data and divided the individual 1660 s peak performance sample analyses into 4 segments of 415 s to simulate a Cr consumption of ~1 μg per individual sample measurement, while SRM 979 standard and baseline measurements were left unchanged (Fig. 4). The reproducibility reached in this test for $\mu^{54}Cr$ of 120 individual sample measurements is 19 ppm (2 sd). This shows that our approach using MC-ICPMS results in comparable precision to measurements of similar amounts of Cr by TIMS, but with MC-ICPMS analysis being significantly faster and yielding additional stable isotope information.

3.5 Acid stepwise dissolution of the Ivuna CI chondrite

As part of the analytical development for the methods presented here, we measured Cr extracted from eleven separates from a stepwise dissolution experiment of the Ivuna CI chondrite that has previously been analysed for the isotopic composition of other elements.[47] The presence of distinct presolar carrier phases of chromium isotopes in primitive chondrites such as Ivuna has been identified in a number of studies using a similar approach, which results in the crude separation of different mineralogical components within a meteorite according to their acid resistance.[1,6,15] Because this produces a wide spread in the isotopic and chemical composition of each step, comparison with previous results for the step wise dissolution provides a good test of our analytical method. In addition, the stable isotope data obtained in our study provide additional information that was previously not available. Because these data were produced as part of the development of the analytical protocol developed here, some of the data have been measured with a lower degree of precision and have larger attached uncertainties (Table 4).

We compare in Fig. 5 our new results for this experiment with previously published Cr isotopic data for the CI chondrite Orgueil obtained by TIMS.[6] Although there are differences in the size of the dissolved sample and the exact number of leaching steps, both datasets follow the same isotopic trends, indicating that the ^{53}Cr and ^{54}Cr obtained by MC-ICPMS and TIMS are comparable. In detail, the higher resolution dissolution experiment employed here displays larger $\mu^{54}Cr$ excesses, whereas the deficits are nearly indistinguishable. The larger excesses may point to a better preservation of the carriers of anomalous ^{54}Cr in Ivuna compared to Orgueil. A better preservation of the ^{54}Cr carrier is also supported by the observation that the $\mu^{53}Cr$

Table 4 Stable and mass-independent Cr isotope data for the step wise dissolution experiment of the CI chondrite Ivuna. Shown uncertainties are the 2 se of the replicate analyses except where stated otherwise. Uncertainties for the calculated bulk composition were determined by Monte Carlo simulation using uncertainties on shown isotope ratios and assuming a 10% uncertainty on the absolute Cr abundance

wt% Cr	Step	δ^{50}Cr	μ^{53}Cr	μ^{54}Cr	n	^{55}Mn/^{52}Cr
<0.1	L1	—	—	—	—	44
0.1	L2	+0.210 ± 0.130	+246 ± 20	−592 ± 17	4	189
14.9	L3	+0.614 ± 0.031	+110.7 ± 2.3	−579 ± 5.2	5	1.79
2.1	L4	+0.829 ± 0.033	+87.5 ± 4.6	−649 ± 10	5	3.86
7.3	L5	+1.346 ± 0.079	+51.4 ± 1.3	−876 ± 10	5	0.58
48.8	L6	+0.795 ± 0.010	+22.4 ± 1.5	−799 ± 2.9	10	0.21
1.4	L7	+0.770 ± 0.064	−11.7 ± 3.9	+3369 ± 19	5	1.27
0.5	L8	+2.052 ± 0.015	+56.4 ± 2.0	+5306 ± 8.7	5	2.47
0.9	L9	+0.538 ± 0.008	−46.0 ± 1.6	+15753 ± 8.5	10	1.53
4.3	L10	+0.807 ± 0.049	−29.4 ± 7.9	+9194 ± 19	5	0.07
7.7	L11	−0.218 ± 0.007	−96.5 ± 0.7	+3353 ± 5.0	4	0.09
11.8	L12	−0.418 ± 0.007	−77.3 ± 8.4	+777 ± 8.8	5	0.11
	Calc. bulk (±2 sd)	+0.590 ± 0.08	+15.0 ± 5.4	413 ± 129		0.73

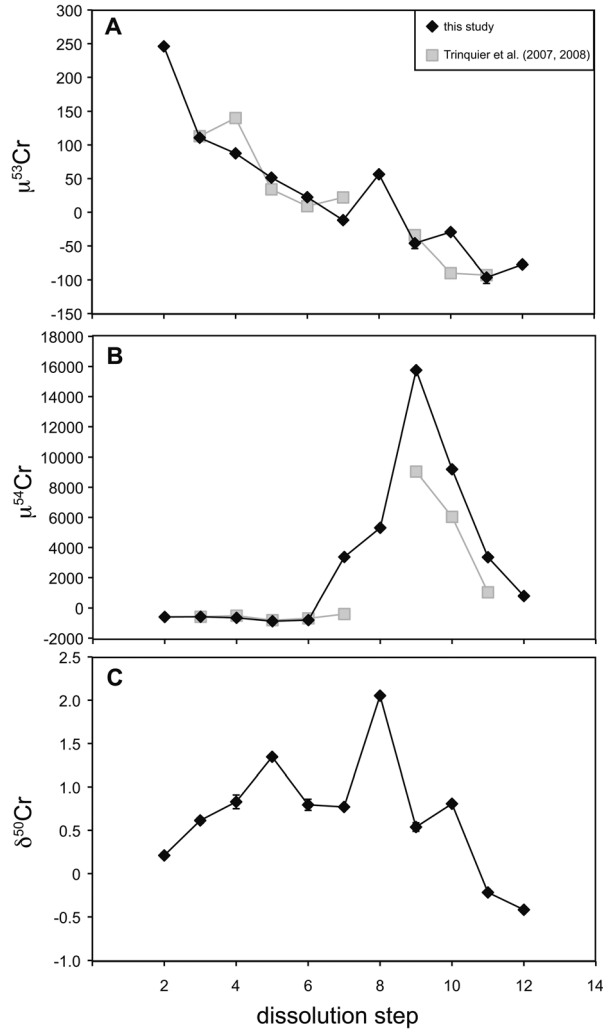

Fig. 5 Shown are the μ^{53}Cr (A), μ^{54}Cr (B), and δ^{50}Cr (C) data for the step wise dissolution experiment of the CI chondrite Ivuna. Detailed information about the applied procedure can be found in Paton *et al.*[47] Similar data for an experiment using the CI chondrite Orgueil from Trinquier *et al.*[6] are also shown for comparison.

data of both meteorites, although measured by different methods, are in excellent agreement with each other. Mass balance calculations further indicate that both μ^{53}Cr and δ^{50}Cr are indistinguishable from those of the bulk measurement. The calculated bulk μ^{54}Cr composition of Ivuna (413 ± 129) is more positive than the measured bulk composition (155.2 ± 4.8). Most likely, this overestimation is caused by inaccuracies in determining the absolute Cr abundance in each leaching step. Because variations in the individual μ^{54}Cr composition of the dissolution steps are more than ten times larger than those of μ^{53}Cr and δ^{50}Cr, the recalculated bulk μ^{54}Cr composition is significantly more susceptible to this effect. Thus, considering the uncertainties involved in reconstituting the bulk composition, the calculated μ^{54}Cr is also in agreement with that of the measured bulk Ivuna.

The stable isotope composition for the individual dissolution steps provides additional information previously not available (Fig. 5C). While the ^{54}Cr data apparently suggest that the nucleosynthetic variability of ^{54}Cr in the solar system is the result of variable contribution of a single carrier phase, the stable isotope data indicate that there are also large stable isotopic variations in the mineral assemblage of Ivuna. Although some of the variations are likely related to partial extraction and fractionation of Cr from a single carrier in different dissolution steps (*e.g.*, steps L2–L5), the observation of reversing trends and individual peaks in the pattern of the dissolution experiment cannot be caused by a single and homogeneous Cr stable isotope composition. In contrast, this observation suggests that multiple carriers of Cr isotopes with diverse stable isotopic composition are present in Ivuna. Such presence of minerals with differences in their stable Cr isotope composition has the potential to explain the Cr stable isotope heterogeneity that exists between bulk solar system reservoirs.[40] In detail, carbonaceous chondrites are on average isotopically lighter than ordinary chondrites and Earth. The dissolution experiment reveals that some of the carriers of isotopically heavy Cr are mineralogically linked with the carriers of ^{54}Cr enrichments (dissolution steps L8–L10). Although a direct correlation of the Cr stable isotopic composition and variable

^{54}Cr enrichment is not apparent from the meteorite data presented here, the presence of large stable isotopic variations in the step wise dissolution of Ivuna that appear to coexist with nucleosynthetic variability suggests that at least in part stable isotopic differences in bulk solar system reservoirs might be a result of the same process that imparted the nucleosynthetic variability in the same reservoirs.

4 Conclusions

In this paper we describe novel analytical protocols for the highly precise and accurate determination of the stable and mass-independent Cr isotopic composition of silicate samples by MC-ICPMS. Our results can be summarized as follows:

(1) Repeat measurements of standards indicate that μ^{53}Cr and μ^{54}Cr can be measured with a precision that is better than 2.5 and 5.8, respectively. Although the method described here consumes substantially more Cr than traditional TIMS analyses, it also allows for a significantly improved (by a factor of at least two) reproducibility. The stable Cr isotope composition obtained concurrently to the mass-independent data has a precision of 0.05‰ Da^{-1}, which is comparable to other studies.

(2) Our high precision data reveal small differences in the mass-independent composition between different Cr standards and BSE when using the kinetic law for mass bias correction. These differences are best explained by the loss of Cr during the production of the standards by equilibrium mass fractionation. This highlights the importance of carefully assessing and stating the Cr isotopic composition of the standard with respect to Earth when making precise measurements of the mass-independent composition.

(3) When comparing data blocks equivalent to 1 μg of Cr consumption a reproducibility of the MC-ICPMS data of 19 ppm for μ^{54}Cr was achieved. This is comparable to the amount of Cr used by traditional TIMS analysis for similar precision, while the MC-ICPMS data also contain stable Cr isotope information and require significantly less time allowing for increased sample throughput.

(4) Stable Cr data for the achondrites Bilanga and NWA 2999 do not agree with the interpretation of Moynier *et al.*[40] that differences in the stable Cr isotope composition of Earth and chondrites are the result of fractionation during metal–silicate differentiation, but suggest, in agreement with the presence of mineralogical phases with distinct Cr stable isotopic composition in the CI chondrite Ivuna, that these differences are predominantly a result of slightly diverse Cr stable isotope compositions of the precursors they accreted from.

(5) Step wise dissolution experiment of the CI chondrite Ivuna demonstrates the advantage of using the MC-ICPMS over the TIMS by revealing previously unknown carriers of large Cr stable isotope variations that co-vary with the known presence of carriers of large mass-independent anomalies.

Acknowledgements

Funding for this project was provided by grants from the Danish National Research Foundation (grant number DNRF97) and from the European Research Council (ERC Consolidator grant agreement 616027-STARDUST2ASTEROIDS) to M.B. We would also like to thank two anonymous reviewers for their thoughtful comments.

References

1 M. Rotaru, J.-L. Birck and C. J. Allègre, *Nature*, 1992, **358**, 465–470.
2 A. S. Ellis, T. M. Johnson and T. D. Bullen, *Science*, 2002, **295**, 2060–2062.
3 R. Frei, C. Gaucher, S. W. Poulton and D. E. Canfield, *Nature*, 2009, **461**, 250–253.
4 D. Fibbi, S. Doumett, L. Lepri, L. Checchini, C. Gonnelli, E. Coppini and M. Del Bubba, *J. Hazard. Mater.*, 2012, **199**, 209–216.
5 G. Lugmair and A. Shukolyukov, *Geochim. Cosmochim. Acta*, 1998, **62**, 2863–2886.
6 A. Trinquier, J.-L. Birck and C. Allegre, *Astrophys. J.*, 2007, **655**, 1179–1185.
7 K. Yamashita, S. Maruyama, A. Yamakawa and E. Nakamura, *Astrophys. J., Lett.*, 2010, **723**, 20.
8 D. Hartmann, S. E. Woosley and M. F. El Eid, *Astrophys. J.*, 1985, **297**, 837–845.
9 B. S. Meyer, T. D. Krishnan and D. D. Clayton, *Astrophys. J.*, 1996, **462**, 825.
10 D. Clayton, *Handbook of Isotopes in the Cosmos: Hydrogen to Gallium*, Cambridge University Press, 2003, vol. 1.
11 N. Dauphas, L. Remusat, J. H. Chen, M. Roskosz, D. A. Papanastassiou, J. Stodolna, Y. Guan, C. Ma and J. M. Eiler, *Astrophys. J.*, 2010, **720**, 1577–1591.
12 L. Qin, L. R. Nittler, C. M. O. Alexander, J. Wang, F. J. Stadermann and R. W. Carlson, *Geochim. Cosmochim. Acta*, 2011, **75**, 629–644.
13 S. E. Woosley and A. Heger, *Rev. Mod. Phys.*, 2002, **74**, 1015–1071.
14 G. Wasserburg, M. Busso, R. Gallino and K. Nollett, *Nucl. Phys. A*, 2006, **777**, 5–69.
15 A. Trinquier, J.-L. Birck, C. J. Allègre, C. Gopel and D. Ulfbeck, *Geochim. Cosmochim. Acta*, 2008, **72**, 5146–5163.
16 F. Moynier, Q.-Z. Yin and B. Jacobsen, *Astrophys. J., Lett.*, 2007, **671**, L181–L183.
17 A. Trinquier, J.-L. Birck and C. J. Allegre, *J. Anal. At. Spectrom.*, 2008, **23**, 1565–1574.
18 L. Qin, C. M. O'D Alexander, R. W. Carlson, M. F. Horan and T. Yokoyama, *Geochim. Cosmochim. Acta*, 2010, **74**, 1122–1145.
19 A. Shukolyukov and G. Lugmair, *Geochim. Cosmochim. Acta*, 2004, **68**, 2875–2888.
20 A. Shukolyukov and G. W. Lugmair, *Earth Planet. Sci. Lett.*, 2006, **250**, 200–213.
21 R. Andreasen and M. Sharma, *Int. J. Mass Spectrom.*, 2009, **285**, 49–57.
22 M. Bizzarro, C. Paton, K. Larsen, M. Schiller, A. Trinquier and D. Ulfbeck, *J. Anal. At. Spectrom.*, 2011, **26**, 565–577.

23 K. K. Larsen, A. Trinquier, C. Paton, M. Schiller, D. Wielandt, M. A. Ivanova, J. N. Connelly, Å. Nordlund, A. N. Krot and M. Bizzarro, *Astrophys. J., Lett.*, 2011, **735**, L37.
24 M. Schiller, J. Baker, J. Creech, C. Paton, M.-A. Millet, A. Irving and M. Bizzarro, *Astrophys. J., Lett.*, 2011, **740**, L22.
25 M. Schiller, C. Paton and M. Bizzarro, *J. Anal. At. Spectrom.*, 2012, **27**, 38–49.
26 M. B. Olsen, M. Schiller, A. N. Krot and M. Bizzarro, *Astrophys. J., Lett.*, 2013, **776**, L1.
27 J. Foriel, F. Moynier, T. Schulz and C. Koeberl, *Meteorit. Planet. Sci.*, 2013, 1–12.
28 T. Inui, W. Abe, M. Kitano and T. Nakamura, *X-Ray Spectrom.*, 2011, **40**, 301–305.
29 A. Pourmand and N. Dauphas, *Talanta*, 2010, **81**, 741–753.
30 S. Weyer and J. B. Schwieters, *Int. J. Mass Spectrom.*, 2003, **226**, 355–368.
31 C. Paton, J. Hellstrom, B. Paul, J. Woodhead and J. Hergt, *J. Anal. At. Spectrom.*, 2011, **26**, 2508.
32 W. R. Shields, T. J. Murphy, E. J. Catanzaro and E. L. Garner, *J. Res. Natl. Bur. Stand., Sect. A*, 1966, **70**, 193–197.
33 K. Kehm, E. H. Hauri, C. M. O. Alexander and R. W. Carlson, *Geochim. Cosmochim. Acta*, 2003, **67**, 2879–2891.
34 I. Platzner, J. V. Sala, F. Mousty, P. R. Trincherini and A. L. Polettini, *J. Anal. At. Spectrom.*, 1994, **9**, 719.
35 I. Leya, M. Schönbächler, U. Wiechert, U. Krähenbühl and A. N. Halliday, *Int. J. Mass Spectrom.*, 2007, **262**, 247–255.
36 H. Balsiger, J. Geiss and M. E. Lipschutz, *Earth Planet. Sci. Lett.*, 1969, **6**, 117–122.
37 P. Taylor, R. Maeck and P. De Bièvre, *Int. J. Mass Spectrom.*, 1992, **121**, 111–125.
38 R. Schönberg, S. Zink, M. Staubwasser and F. von Blanckenburg, *Chem. Geol.*, 2008, **249**, 294–306.
39 L. Halicz, L. Yang, N. Teplyakov, A. Burg, R. Sturgeon and Y. Kolodny, *J. Anal. At. Spectrom.*, 2008, **23**, 1622.
40 F. Moynier, Q.-Z. Yin and E. Schauble, *Science*, 2011, **331**, 1417–1420.
41 M. Wadhwa, *Rev. Mineral. Geochem.*, 2008, 493–510.
42 I. H. Campbell, H. St and C. O'Neill, *Nature*, 2012, **483**, 553–558.
43 E. D. Young, A. Galy and H. Nagahara, *Geochim. Cosmochim. Acta*, 2002, **66**, 1095–1104.
44 J.-L. Birck and C. J. Allègre, *Earth Planet. Sci. Lett.*, 1984, **11**, 943–946.
45 A. Yamakawa, K. Yamashita, A. Makishima and E. Nakamura, *Astrophys. J.*, 2010, **720**, 150–154.
46 K. Keil, *Chem. Erde – Geochem.*, 2012, **72**, 191–218.
47 C. Paton, M. Schiller and M. Bizzarro, *Astrophys. J., Lett.*, 2013, **763**, L40.

